International Journal of Engineering Research and Development

DOI: 10.29137/ijerad.1339973

Volume:17 Issue:02 Pages:498-508 July/2025

Research Article

Investigation of Effects Different Particle Size Quartz and Feldspar on Body Physical Properties

Emine Zülal Çakar[1], **Atamer Akbay** [1], **Orçun Zırtıl** [1] **İrem Altınok** [1]

[1]Çanakcılar Ceramic Industry And Trade Inc. Gökçebey, 67670, Zonguldak, Türkiye

Received: 05/05/2024 **Accepted**: 12/06/2024 **Published Online:** 15/07/2025
Final Version: 01/07/2025

Abstract

Ceramic sanitary ware is produced using raw materials such as inorganic non-metallic feldspar, quartz, clay, and kaolin. These raw materials are prepared as a slurry according to a specific recipe. Plaster and/or resin are then shaped in molds to create designs for sinks, pedestals, toilet bowls, cisterns, bidets, latrine stones, urinals, and shower trays. They are hard-structured, opaque, low-porosity materials obtained by firing at 1200-1250 ℃. Two types of materials are used in the production of ceramic sanitary ware: cored and non-cored (hard). Coreless raw materials are broken down by various methods to reduce the grain size. The grinding process of silica sand and feldspar, which are the coreless raw materials within vitrified ceramics, consumes the most energy after firing. This study was carried out to investigate the effects of the grain size of silica sand and feldspar on the physical properties of the prepared bodies. For this purpose, slurry was prepared using mill phases with varying grinding times. To examine the physical properties of the prepared slurries, such as shrinkage, deformation, and water absorption, they were fired in a tunnel kiln at 1210 °c for approximately 17 hours. The XRD graph was analysed to reveal the effect of grain size on the phases within the structure and the formation of the glassy phase. The study observed that as the grinding time increased, meaning that the grain size of the body became finer, water absorption decreased while dry strength and firing shrinkage increased. According to the results of the mineralogical analysis, it was found that the free quartz ratio decreased with the reduced grain size.

Keywords

Sanitaryware, Hard raw material, Grinding, Casting properties, Vitrous china

*** Corresponding Author:** *e.kazli@creavit.com.tr*

1. Introduction

Ceramic sanitary wares are dense, opaque, and low-porosity materials produced by shaping a slurry—prepared from inorganic and non-metallic raw materials such as feldspar, quartz, clay, and kaolin according to a specific formulation—into molds made of plaster and/or resin for items including sinks, pedestals, toilet bowls, cisterns, bidets, squat pans, urinals, and shower trays, followed by firing at high temperatures ranging from 1200 to 1250 °C (Yener, 2000; Dağ, 2009).

Ceramics are generally classified into two categories: traditional and advanced ceramics. Since sanitary wares are composed of clay, kaolin, quartz, and feldspathic raw materials, they fall under the category of traditional ceramics (Kingery, 1960). Clay minerals, which consist of layered and/or chained structures of silica and alumina, are fine-grained materials used to impart plasticity and green strength to the ceramic body (Dağ, 2009; Fortuna, 2000a). Kaolins are formed by the weathering and dehydration of feldspathic rocks, and due to their short transportation distance, they are generally purer and cleaner than clays. Kaolins contribute to the high-temperature deformation resistance of the ceramic body (Fortuna, 2000a).

In sanitary ware production, the most influential parameters are the physical and chemical properties of the raw materials. Among the constituents of the slip formulation, clays possess the finest particle size distribution, whereas feldspar and quartz are coarser and significantly harder materials. These dimensional properties play a critical role throughout the manufacturing process, including slip preparation, glazing, and firing stages (Heckroodt, 1990).

The particle size distribution of raw materials and the resulting microstructure of the ceramic body significantly affect physical properties such as deformation, mechanical strength, and water absorption. Due to its coarse-grain structure, quartz enhances crack resistance during drying. When quartz interacts with feldspathic phases, it contributes to the formation of mullite, which imparts deformation resistance to the ceramic body. However, larger quartz grains fail to participate effectively in this interaction and remain as free quartz. For an optimum vitrified structure, 40–50% of the quartz particle size distribution must be smaller than 10 µm. This is attributed to the fact that finer quartz particles melt more easily and rapidly, thereby facilitating the formation of a glassy phase and improving control over the flowability of the slip (Stathis, 2004; Umucu, 2014; Haner, 2021; Dağ, 2009; Fortuna, 2000).

In previous studies on porcelain bodies with varying quartz particle sizes, three different quartz fractions (10, 45, and 63 µm) were evaluated. As particle size decreased, an increase in firing shrinkage and mechanical strength was observed, while no significant changes were detected in water absorption or bulk density (Yıldızay, 2020). In another study, it was reported that by increasing the grinding time of hard raw materials used in sanitary porcelain production, it was possible to reduce the firing temperature while achieving water absorption below 0.5% and mechanical strength values exceeding 400 kg/cm² (Özel et al., 2011).

In a study involving albite and silica sand ground separately using wet milling for various durations, a slip prepared with silica sand (D_{50} = 13.2 µm) and albite (D_{50} = 10.6 µm) yielded satisfactory results and provided an energy saving of approximately 27% during slip preparation (Kara, 2022).

Industrially, the production of casting slips involves the wet milling of non-plastic (hard) raw materials in alumina ball mills, followed by blending with plastic materials. The grinding stage is the most energy-intensive step within the slip preparation process, especially as particle size decreases, due to the increased fracture resistance of finer particles. Thus, as particle size is reduced, grinding time and, consequently, energy consumption increase significantly (Gao, 1993). Therefore, in order to minimise energy use while maintaining the desired physical properties, it is essential to utilise the largest possible particle size that still meets product requirements.

In a study on ceramic tiles, it was reported that increasing the grinding duration led to a finer particle size distribution, which in turn improved the mechanical strength and shrinkage of the body, while reducing water absorption (Kartal et al., 2001). Similarly, a study investigating the effects of particle size distribution on the properties of vitrified ceramic bodies showed that as the particle size became finer with prolonged grinding, physical characteristics of the slip changed significantly (Sabutay, 1998).

In this context, the present study aims to investigate the effects of silica sand and feldspar with varying particle sizes on the physical properties of vitrified ceramic (vitreous china) bodies. Silica sand and sodium feldspar were wet milled for different durations using an alumina ball mill, and their particle size distributions were analysed. Subsequently, slips were prepared by combining each milling fraction with fixed amounts of clay and kaolin. The casting behaviour and particle size distribution of the slips were systematically evaluated.

2. Materials and Methods

2.1. Raw Materials

The raw materials used in this study include silica sand sourced from the Şile region and sodium feldspar obtained from the Çine region. The clay and kaolin used in the plastic phase are identical in type and quantity across all formulations. Sieve residue analyses of the raw materials were performed using a Retsch AS200 model sieve shaker. Due to the coarse particle size of the materials, particle size distribution was not evaluated using laser diffraction methods. The sieve residue results for silica sand and sodium feldspar are presented in Table 1. It was observed that the majority of silica sand particles remained on the 90-micron sieve, while the sodium feldspar showed a dominant fraction retained above the 250-micron sieve.

Table 1. Sieve Residue Analysis of Silica Sand and Sodium Feldspar

Raw Material	+250	+90	+63	+45	+32	Total
Sodium Feldspar	64,54	20,46	4,81	2,71	1,13	100
Silica Sand	3,86	72,02	6,47	0,6	0,33	100

2.2. Recipe

The formulation used in the experiments contains 30% feldspar and 18% silica sand. The remaining proportion is distributed between kaolin and clay. In the prepared bodies, kaolin is incorporated into the milling phase to prevent the sedimentation of sodium feldspar and silica sand. The composition ratios of the formulation are presented in Table 2.

Table 2. The Formulation Used in the Study

Phase	Raw Material	Recipe Ratios
Mill Phase	Sodium Feldspar	%30
	Silica Sand	%18
	Kaolin	%4
Fluxing Phase	Clay/Kaolin	%48

2.3. Body Optimization Studies

During the preparation of the developed body formulations, the moisture content of the raw materials was taken into consideration. The raw materials, along with the required amounts of water and electrolyte, were loaded into ball mills. The milling was carried out in a silex-lined ball mill with a solid capacity of 250 kg, using alumina grinding media in three different sizes: 50 mm, 30 mm, and 20 mm in diameter. The particle size distribution of the milled slurry was analysed using a Malvern Master Sizer 2000 via laser diffraction, and sieve residue analysis was also conducted for additional verification. The solid concentration of the vitreous slips was adjusted to 72%, and the slurry density was maintained at approximately 1800 g/L. The viscosity values of the prepared slips were measured using a Gallenkamp viscometer and a Brookfield LVDV-II+P model viscometer. Following a one-day aging period, the slips were shaped using plaster molds. The shaped specimens were first air-dried at room temperature for 12 hours, then oven-dried at 105 ± 5 °C for 24 hours. In addition to laboratory test plates, wall-hung toilet bowls were also cast to evaluate casting performance in greater detail. Both the plates and the sanitary ware products were fired at 1210 °C for 17 hours in a tunnel kiln located within the vitreous ceramics production line of Çanakcılar Seramik A.Ş.The grinding durations applied in the ball mill were 2, 3, and 4.5 hours, as detailed in Table 3. It is well known that as particle size decreases, the resistance of particles to fracture increases (Gao, 1993). In this study, it was observed that the grinding time increased as the raw materials were reduced from coarse to finer particle sizes.

Table 3. Grinding Durations Applied in the Ball Mills

Sample	Duration
D1	2 hours
D2	3 hours
D3	4 hours 30 minutes

Particle size distribution measurements were performed using a Malvern Master Sizer 2000 device. The target particle sizes for the silica sand and sodium feldspar loaded into the mill were set to 75, 55, and 45 microns. The desired particle size distributions, specifically the d(90) values, were successfully achieved as presented in Table 4. As shown in Distribution Graph 1, the accumulation of particle clusters is evident. The particle sizes below 1 micron are primarily attributed to the clay and kaolin components, and thus exhibit similar distributions.

Table 4. Particle Size Distribution Analysis of the Milling Phase in the Study

Sample	D(10)	D(50)	D(90)
D1	2,218	22,897	74,567
D2	1,939	17,991	61,233
D3	1,780	13,753	43,902

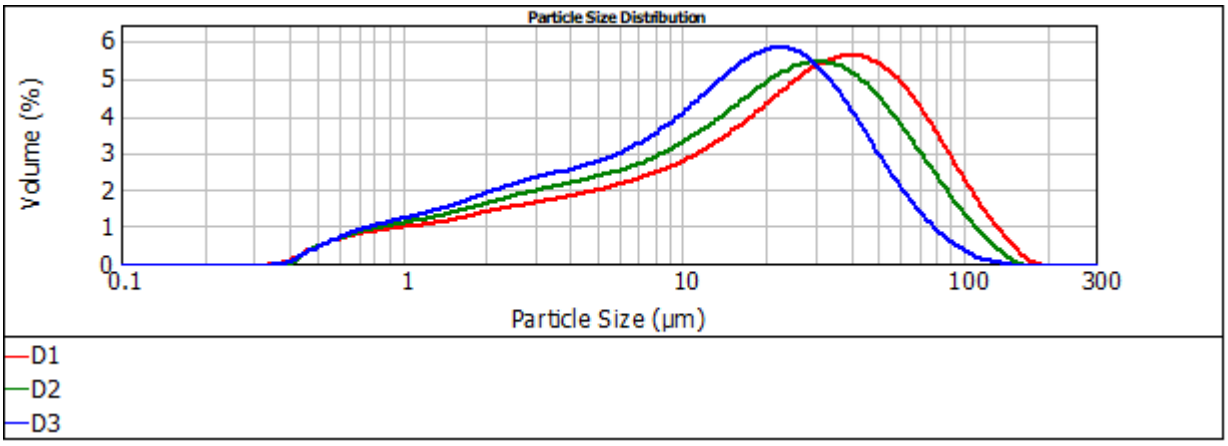

Figure 1. Particle Size Distribution of the Milling Phase Used in the Experiments

When the residues corresponding to the milling durations given in Table 5 were examined, it was observed that the reduction was not linear. The sieve residues below 32 microns were determined as 25.96%, 17.28%, and 3.98%, respectively.

Table 5. Sieve Residue Percentage of the Milling Phase Used in the Experiments

Sample/Micron	+90	+63	+45	+32	Total
D1	0,8	4,45	11,19	9,52	25,96
D2	0,98	2,74	5,83	7,73	17,28
D3	2,0	1,45	0,42	0,11	3,98

Following the milling process, clay and kaolin were added to the fluxing phase for body preparation. The physical property measurements of the prepared slips are presented in Table 6. The slips were adjusted to a specific gravity of 1800 g/L, and their viscosity values were found to be nearly identical. The thickness gain after 1 hour was also consistent across all samples. However, the Baroid-type thickness gain was higher in the coarse-grained slip (D1). Additionally, the initial torsion value (Torsion 1), which reflects the first flow resistance, was higher in the fine-grained slip. These results indicate that the coarse-grained slip exhibits a more viscous structure compared to the fine-grained slip.

Table 6. Body Preparation Parameters Used in the Experiments

Parameters	D1	D2	D3
Density (g/L)	1800	1800	1800
Viscosity (cP)	483	463	457
Torsion 1	310	315	320
Torsion 2	245	250	260

Table 6 (continued). Body Preparation Parameters Used in the Experiments

Parameters	D1	D2	D3
Torsion Difference	65	65	60
Thickness (mm/h)	7,7	7,7	7,7
Baroid Thickness (mm)	9,4	9,3	9,3

3. Characterisation

Shrinkage Measurement:
After the casting process, a 100 mm reference mark is drawn on the surface of the test plate using a calliper. The length after oven drying is recorded as value (A), and the length after firing is recorded as value (B). The total shrinkage is then calculated using the following formula:

$$Drying\ Shrinkage\ (\%) = 100 - A \quad (1)$$

$$Firing\ Shrinkage(\%) = Total\ Shrinkage - Drying\ Shrinkage \quad (2)$$

$$Total\ Shrinkage\ (\%) = 100 - B \quad (3)$$

Deformation Measurement:
A 25 cm rod is placed such that half of its length is suspended between two supports and then subjected to firing. After firing, the deviation is measured by referencing the unsupported section of the rod on a graph paper to assess any deformation.

Water Absorption Measurement:
Fired ceramic plates are first brought to constant weight and weighed (T1). The samples are then placed into a water tank, and the water is heated to 100 °C. After maintaining this temperature for 2 hours, the samples are allowed to cool and are subsequently left immersed in water for an additional 20 hours. After immersion, the plates are removed, surface-dried, and reweighed (T2). Water absorption (%) is calculated using the following formula:

$$Water\ Absorption\ (\%) = \frac{T2-T1}{T1} * 100 \quad (4)$$

Dry Strength Measurement:
Dried test bars with a length of 25 mm were subjected to fracture testing using a Netzsch Tester 40 under a load of 150 N. The width (b) and height (h) of the fractured bars were measured using a calliper. The fracture load (A), corresponding to the applied 150 N force, and the support span (B) were recorded from the testing device. Dry strength was calculated using the following formula:

$$Dry\ Strength\ (\frac{kgN}{cm^2}) = \frac{A*B}{40*(h^2*\frac{b}{6})} \quad (5)$$

As with the milling phase, the prepared slips were subjected to particle size distribution and sieve residue analyses. The particle size distribution results are presented in Table 7. The d(90) values of the fluxing phase particles were determined to be 57.434 µm, 46.354 µm, and 37.885 µm, respectively.

Table 7. Particle Size Distribution Analysis of the Fluxing Phase in the Study

Sample	D(10)	D(50)	D(90)
D1	1,189	11,808	57,434
D2	1,607	10,343	46,354
D3	1,530	9,277	37,885

As shown in Table 8, it was observed that the fraction below 63 microns was predominant in the D1 sample (coarser-grained), while the fraction above 90 microns was higher in the D3 sample (finer-grained). This observation is attributed to the shorter milling duration.

Table 8. Sieve Residue Percentage of the Fluxing Phase Used in the Experiments

Sample	+90	+63	+45	+32	Total
D1	0,39	2,79	6,39	4,66	14,23
D2	0,45	1,80	4,37	3,09	9,71
D3	2,97	2,2	0,5	0,17	5,85

Slips prepared from the formulated compositions were cast into plaster molds. After demolding, the cast plates were left to rest for 12 hours and subsequently dried in an oven at 105 ± 5 °C for 24 hours. The results of the physical property measurements are presented in Table 9.

Table 9. Physical Test Results of the Study

Parametre	D1	D2	D3
Drying Shrinkage (%)	2,5	2,5	2,5
Firing Shrinkage (%)	8,5	8,6	8,9
Firing Shrinkage (%)	11	11,1	11,4
Deformation (mm)	28	26	27
Water Absorbtion (%)	0,47	0,20	0,01
Dry Strength (kgN/cm^2)	27,48	29,90	32,26

As shown in Figure 2, drying shrinkage was not significantly affected by variations in particle size distribution. However, firing shrinkage increased as the particle size of the body decreased. This behaviour is attributed to the fact that finer particles tend to form a glassy phase more easily during firing. Since the drying shrinkage remained relatively constant across all samples, the total shrinkage values of the ceramic bodies varied primarily due to differences in firing shrinkage.

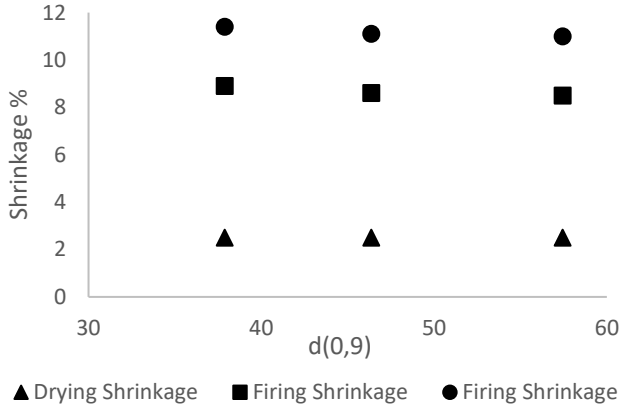

Figure 2. Shrinkage Values for Different Particle Size Distributions

As shown in Figure 3, no significant difference was observed in firing deformation. A clear change in deformation values was not detected. This may be attributed to potential gaps or inconsistencies that occurred during the placement of the test bars between the two support blocks.

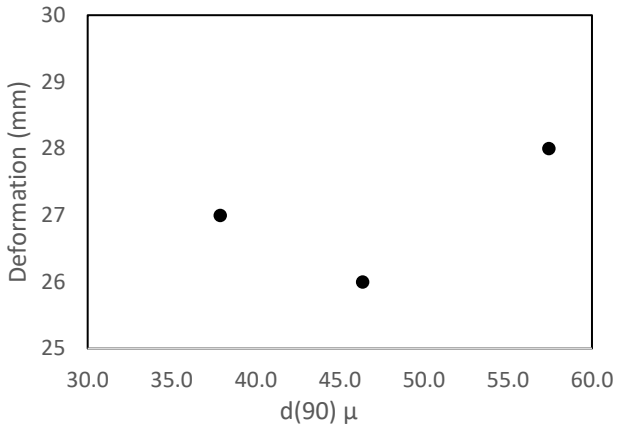

Figure 3. Deformation Values for Different Particle Size Distributions

As shown in Figure 4, the water absorption test is used to assess the pore volume between particles within the ceramic body. A decrease in porosity leads to a corresponding reduction in water absorption. In this study, it was observed that water absorption values decreased as particle size became finer. The D1 sample, which had the coarsest particle size distribution (d90: 57.434 µm), exhibited a water absorption value of 0.47%. It is well established that the maximum allowable water absorption for vitreous ceramic bodies is 0.5%. Therefore, the D1 sample was deemed unsuitable, as it reached the upper limit of the acceptable range.,

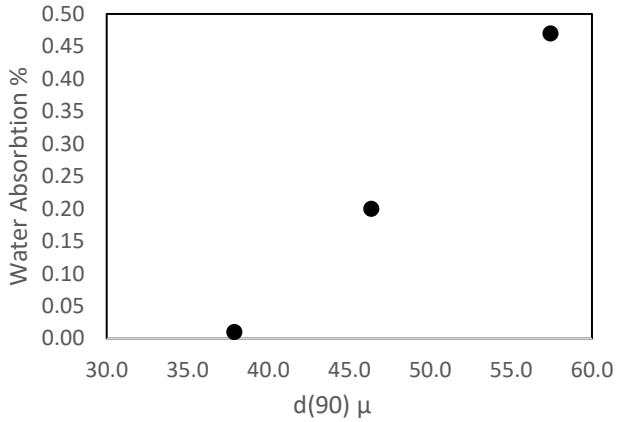

Figure 4. Water Absorption Values for Different Particle Size Distributions

As shown in Figure 5, dry strength—i.e., the resistance of the ceramic body to compressive force—increases as the proportion of fine particles in the body rises, due to the resulting reduction in porosity. In this study, the D1 sample (d90: 57.434 µm) exhibited a dry strength of 27.48 kgN/cm², whereas the D3 sample (d90: 37.885 µm) reached 32.26 kgN/cm². Accordingly, refining the particle size distribution from d90 = 50–60 µm to d90 = 35–40 µm resulted in a 17% increase in dry strength.

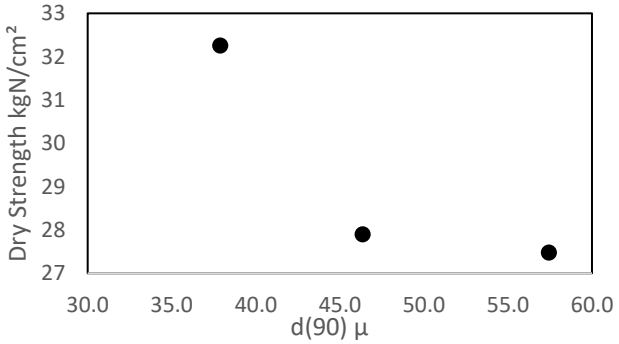

Figure 5. Dry Strength Values for Different Particle Size Distributions

Thermal Expansion Analysis:
Thermal expansion measurements were carried out using a Netzsch DIL 402 PC dilatometer. This analysis evaluates the dimensional change of a material in response to increasing temperature. Thermal expansion values are generally expressed in terms of the linear thermal expansion coefficient (α).

Samples fired in the industrial tunnel kiln were prepared for measurement by wet cutting to approximate dimensions of ~50 mm in length, ~5 mm in width, and ~5 mm in thickness. The specimens were dried in an oven at 105 ± 5 °C. A standard heating schedule was applied to the samples, involving a heating rate of 10 °C/min up to 1000 °C.

Upon examining the results presented in Table 10, it was observed that the thermal expansion values increased as the particle size distribution became finer. As illustrated in Figure 6, α values within the 500–600 °C range indicate that quartz expansion intensified with decreasing particle size. These results suggest that melting initiates earlier as particle size decreases. Finer particle sizes thus offer an advantage for lower-temperature firing of ceramic bodies.

Table10. Results of Thermal Expansion Analysis

^{o}C / dL/L_o*10^{-3}	D1	D2	D3
α 200	5,99	6,25	6,12
α 300	6,16	6,44	6,41
α 400	6,36	6,65	6,69
α 500	6,58	6,88	6,99
α 600	7,23	7,53	7,67
α 700	6,89	7,15	7,25
α 800	6,64	6,82	6,94
α 900	6,62	6,77	6,93
α 1000	6,42	6,64	6,82

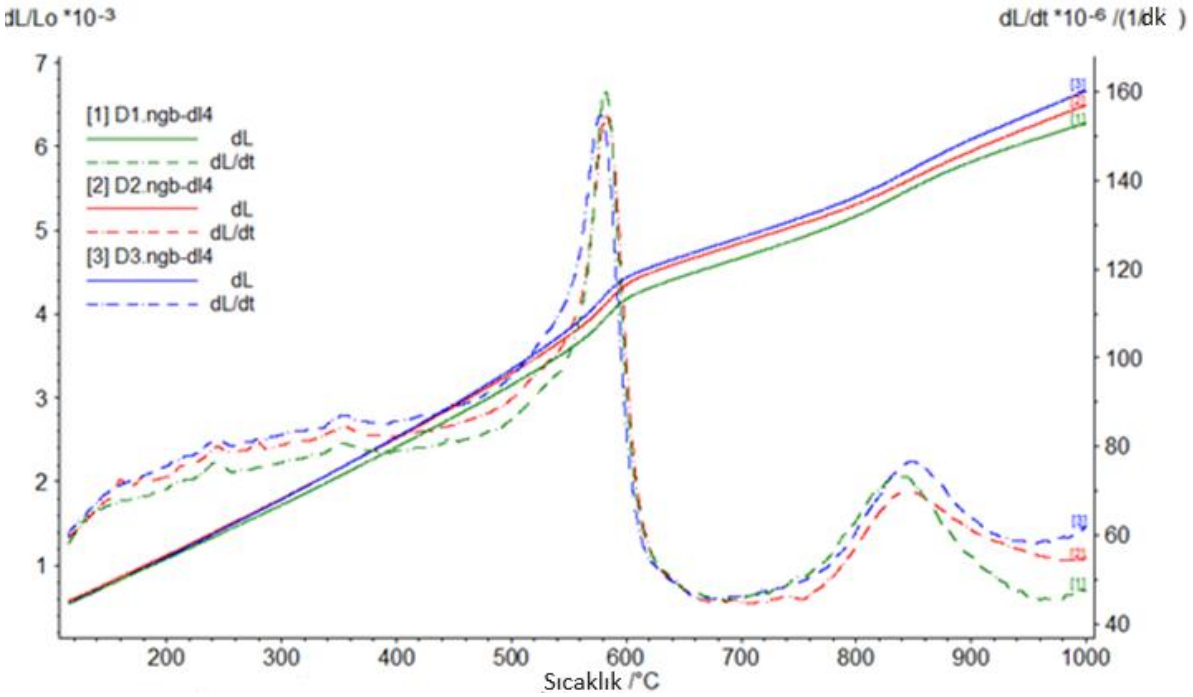

Figure 6. Thermal Expansion Curves from the Study

Mineralogical Characterisation

The crystalline structures of the solids and the corresponding phases present within them were identified using the X-ray Diffraction (XRD) method. For the measurements, the samples were first ground using a tungsten ring mill to achieve a particle size below 63 µm

and then dried in an oven at 105 ± 5 °C. The prepared samples were analysed using a Rigaku Miniflex 600 model XRD device following the appropriate measurement protocol. The phase diagrams of the ceramic bodies are presented in Figure 7. In the phase analysis, the peak observed at 20° 2θ corresponds to free quartz, while the peaks between 20° and 30° 2θ represent mullite and free quartz phases. The D1 sample (d90: 57.434 µm) exhibited the highest free quartz peak intensity at 18%, indicating that it contains the greatest amount of free quartz among all formulations. The relative proportion of the glassy phase decreased in the order of D3 > D2 > D1.

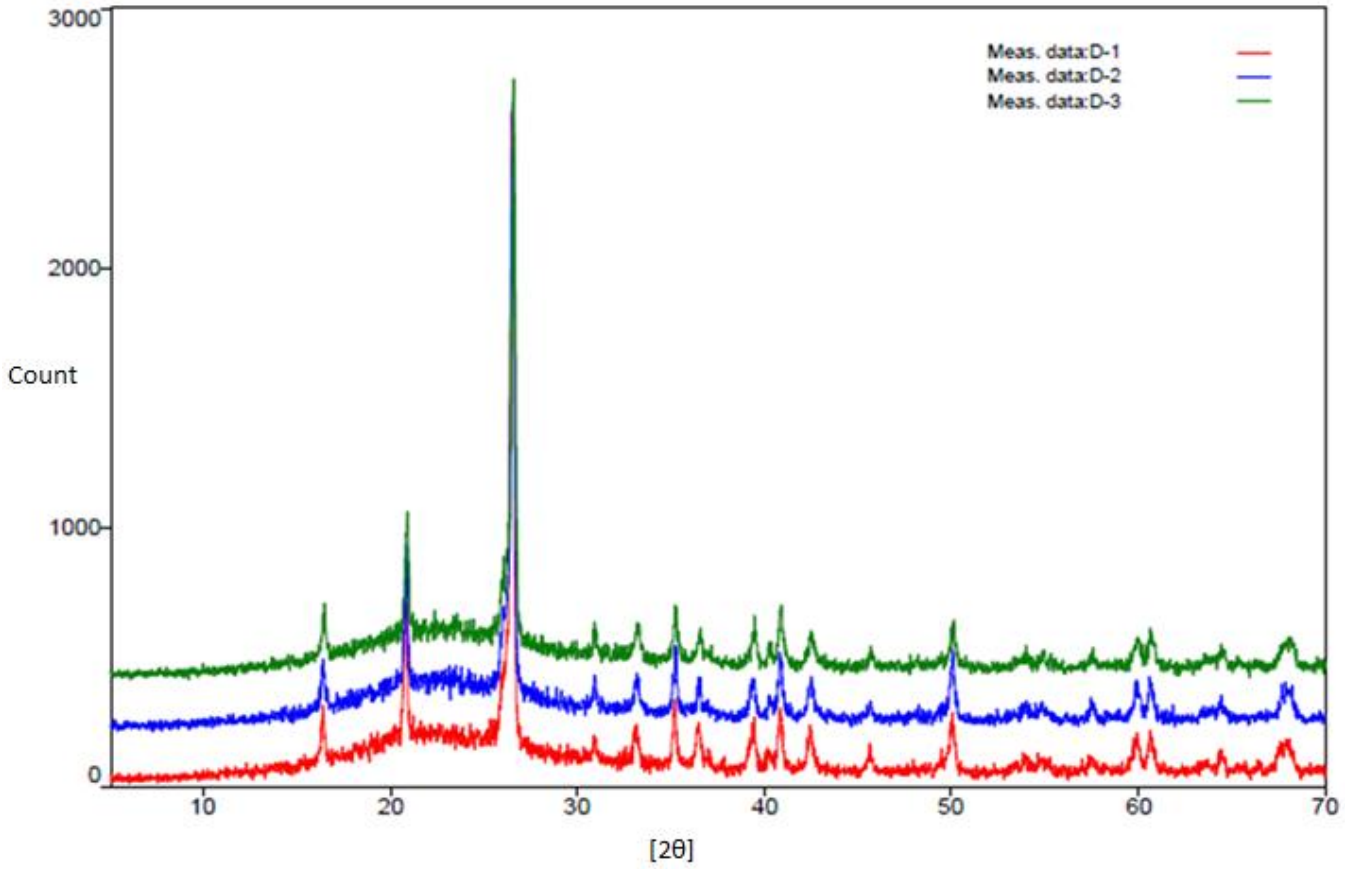

Figure 7. XRD patterns of the samples

4. Results and Discussion

Due to the high cost of quartz used in vitreous ceramic bodies, silica sand—an unprocessed (unground) raw material with a lower purity level than quartz—is preferred as an alternative. This hard and coarse material is ground in ball mills to prepare ceramic slips. In this study, the changes in physical properties of ceramic slips with different particle size distributions obtained through varying milling durations were investigated. It was observed that as the particle size of the slip decreased, both firing shrinkage and compressive strength increased, while water absorption decreased due to the reduction in pore diameter. No significant difference was detected in firing deformation among the samples. Although a reduction in wall thickness development was expected with finer particle sizes, similar thickness values were obtained across all samples. In thermal expansion analysis, the fine-grained bodies exhibited higher expansion values compared to the coarse-grained ones. As the particle size decreases, the surface area increases, leading to greater thermal expansion. Based on all these findings, it is suggested that in the next stage of the research, reducing the particle size distribution of the ceramic body may enable a decrease in the required firing temperature.

5. References

Dağ, P. (2009). Sağlık gereçlerinde kompozisyon değişimlerinin sinterleme üzerine etkileri [Yüksek lisans tezi, Anadolu Üniversitesi]. Fen Bilimleri Enstitüsü, Seramik Mühendisliği Anabilim Dalı.

Fortuna, D. (2000). Ceramic technology sanitaryware. Graphic Line.

Gao, M., & Forssberg, E. W. (1993). A study on the effect of parameters in stirred ball milling. International Journal of Mineral

Processing, 37, 45–59.

Haner, S. (2021). Kuvars kumunun kırılma hızının tanımlanmasında öğütücü ortam boyutunun etkisinin araştırılması. Avrupa Bilim ve Teknoloji Dergisi, 23, 547–551.

Kartal, A., Kurt, Z., & A. (2004). Tane boyutunun massenin ve ürünün fiziksel özellikleri üzerine etkileri. Afyon Kocatepe Üniversitesi Fen Bilimleri Dergisi, 4(1–2), 7–15.

Kara, E., and Çuhadaroğlu, A. D. (2022). Seramik hammaddelerinin ayrı öğütülmesinin etkilerinin incelenmesi. Teknik Bilimler Dergisi, 12(2), 6–11.

Kingery, W. D., Bowen, H. K., & Uhlmann, D. R. (1960). Developments of microstructure in ceramics. In E. Burke, B. Cahlmers, & J. A. Krumhansl (Eds.), Introduction to Ceramics (pp. 265–581). Wiley Series on the Science and Technology of Materials.

Özel, E., Tunçel, D. Y., & Kara, M. K. (2011). Sert hammadde tane boyutunun sağlık gereçleri porseleninin fiziksel özelliklerine etkisi. Gazi Üniversitesi Mühendislik-Mimarlık Fakültesi Dergisi, 26(2), 299–306.

Sabutay, N. (1998). Vitrifiye malzemelerde tane boyut dağılımının ürün özelliklerine etkisi [Yüksek lisans tezi, Anadolu Üniversitesi]. Seramik Mühendisliği Anabilim Dalı.

Stathis, G., Ekonomakou, A., Stournaras, J., & Ftikos, C. (2004). Effect of firing temperature, quartz grain size and content on bending strength and microstructure of sanitary porcelain. Journal of the European Ceramic Society, 24, 2357–2366.

Umucu, Y., & Deniz, V. (2014). The evaluation of grinding behaviors of quartz and feldspar. The Online Journal of Science and Technology, 4(1).

Yener, S. (2000). Kapiler seramik filtre üretiminde doğal zeolit ve kurşun-borlu frit kullanımı [Yüksek lisans tezi, Dumlupınar Üniversitesi]. Seramik Mühendisliği Anabilim Dalı.

Yıldızay, H. (2020, Eylül). Farklı boyutlardaki kuvarsın ilavesinin sert porselen bünyesindeki etkileri. 8. Uluslararası Bilimsel Araştırmalar Kongresi - Fen ve Mühendislik Bilimleri, Türkiye.